Journal of International Scientific Publications:
Materials, Methods & Technologies, Volume 5, Part 2
ISSN 1313-2539, Published at: http://www.science-journals.eu

THE STRUCTURAL AND PHASE STATE FORMED IN CONSTRUCTION TITANIUM ALLOY BY RADIAL FORGING

Galina V. Shlyakhova[1], Vladimir I. Danilov[1], Aleksandr S. Zavodchikov[2],
Dina V. Orlova[1], Lev B. Zuev[1]
[1]Institute of Strength Physics and Materials Science SB RAS, 634021 Tomsk, Russia
[2]Perm State Technical University, 614990 Perm, Russia

Abstract

The feasibility of rod manufacture from construction titanium alloy using radial forging on a high-duty machine SXK16 was investigated. The investigations were carried on for titanium rod samples using the methods of metallography, electron transmission microscophy and X-ray analysis. The results obtained are described herein. It is found that radial forging results in the formation of homogeneous fine-grained structure.Using radial forging process, high-quality items are produced. As-worked material has submicrocrystalline globular structure and an optimal α:β phase ratio. Besides, the technology is more cost-effective relative to conventional flow charts.

Key words: *forging, titanium alloy, fine-grain structure, substructure, pore size*

1. INTRODUCTION

Stringent requirements are imposed on modern construction materials to suit the increasing demand for constructions, which have low specific weight and combine high structural strength and high safety margin. In particular, titanium base alloys have high specific strength combined with high ductility and high corrosion resistance; therefore, these materials enjoy wide use in various branches of industry (Ilyin and co-workers, 2009, Muravyov and co-workers, 2009, Jaffee, 1958). Additional requirements imposed on these alloys are high fatigue and high wear resistance; besides, these materials have to withstand extreme conditions, e.g. dynamic and repetitive alternating loading. And last but not least, high-strength zirconium alloys should have satisfactory formability, in particular, by the manufacture of semi-finished and end products. The above problems can be best approached by the use of severe plastic deformation to form submicrocrystalline structure in metals and alloys having grain size < 1 μm (Bratukhin, 2009, Shorokhov and co-workers, 2006).

The investigations were carried on for titanium alloy containing α- and β-phases, which is employed for the manufacture of hardware for the aircraft industry using cold upset process (see, e.g. Ilyin and co-workers, 2009, Muravyov and co-workers, 2009). It is required that a material from which hardware is produced by cold-work combine satisfactory formability with sufficient strength. To meet these requirements, strict quality control is exerted for the billets to be worked by cold upsetting, i.e. the material's porosity, degree of grain structure dispersion and β-phase content are determined. Traditional processes employed for billet manufacture involve hot rolling on a section mill and secondary machining operations performed on the billet to provide a low-porosity billet having fine grain structure. However, these processes have a grave disadvantage: the gas-saturated and oxide layers have to be removed from the billets, which results in significant processing loss.

Therefore, the process of cold radial forging might be an alternative to billet manufacture processes employing hot rolling and subsequent cold upsetting. In principle, the material treated by severe plastic deformation on modern radial-forging machines would acquire a submicrocrystalline structure,

enhanced strength and a greater degree of plasticity relative to the original material. Besides, the rods produced from this material by cold radial forging have high-quality surface, which requires no secondary machining operations (Bratukhin, 2009).

2. MATERIAL AND INVESTIGATION METHODS

The studied material is a high-strength titanium alloy of martensite type, which undergoes thermal hardening. The alloy has a conventional coefficient of β-phase stabilization equal to 0.8 (see, e.g. Collings, 1984); its chemical composition is presented in Table 1. The evolution of grain-submicrograin structure and the phase composition of material within the deformation nuclei were examined for test samples of titanium alloy rods produced by cold radial forging after each pass, i.e. ∅20→∅16 mm and ∅16→∅10 mm.

Table 1. Chemical composition of the alloy (% by weight)

Al	Mo	V	C	N	Fe	Si	H_2	O_2	Ti
3.3	4.6	4.5	0.05	0.01	< 0.01	≤ 0.10	0.007	0.14	Remainder

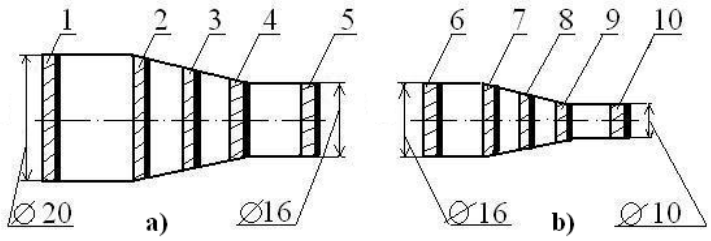

Fig. 1. Passes ∅20→∅16 mm (a) and ∅16→∅10 mm (b) by radial forging and a scheme of cutting of samples **1-10**

Figure 1 shows the scheme of cutting test samples from the deformation nuclei, the sample number increasing with the shrinkage (see Table 2). The areas described by the bold lines correspond to sections prepared for metallographic examination using a standard procedure. First non-etched sections were examined by optical metallographic method (a Neophot-21 microscope); then the same sections were etched using aqueous solution of hydrofluoric (3%) and nitrous acid (3%) (see, e.g. Beckert and Klemm, 1984). Examination of the test samples was also performed by the methods of electron microscopy and X-ray diffraction analysis.

The grain-submicrograin structure of the alloy was investigated by the thin-foil method (see, e.g. Tomas and Goringe, 1979) on an electron microscope EM-125 with the accelerating voltage 125 kV. The foils were cut out of the metallographic sections. The X-ray diffraction analysis was performed for the samples which had been cut out in accordance with the scheme illustrated in Fig. 1. The sections were polished electrochemically to relieve the internal stresses that had built up during the preparation of sections and to remove oxides from the section surface. An X-ray phase analysis was performed in accordance with the Bragg-Brentano scheme ($\theta - 2\theta$) in the interval of angles $10^0 < \theta < 125^0$ (see, e.g. Guinier 1956); the recording was carried on by 0.1^0 steps with the exposition of 5 s per point on a DRON-3 diffractometer operating in Cu K_α radiation with K_β filter. The decoding of diffraction images was performed on a 'Crystallographica Search-Match' device (Version 3. 1. 0. 0).

ISSN 1313-2539, Published at: http://www.science-journals.eu

Table 2. Material porosity and grain size vs shrinkage

Sample No.	Shrinkage, *K*, %	Pore density, mm^{-2}		Maximal pore size, μm		Grain size (arbitrary units)	
		Along billet axis	In the near-surface layer	Along billet axis	In the near-surface layer	Along billet axis	In the near-surface layer
1	0	771	325	18	3.5	6	4
3	17	542	274	9	3	5-4	3
5	20	362	244	2.5	3	4	3-2
7	23	297	202	2	2	3-2	2-1
8	38	183	149	1.5	1	2	1
10	50	102	98	<1	1	2	1

3. DISCUSSION OF RESULTS

3.1. Metallographic analysis

It is found that the non-etched sample **1** has the highest porosity and loose texture along the central portion; evidently, the large-sized non-equiaxial pores had formed at the previous process stages (Fig. 2 a and b). The pore density in the near surface layer of the billet is significantly lower relative to the central portion, with the pores having oval shape and sizes 0.2…0.5 mm. After two passes of radial forging, the material porosity grows less in the rod bulk, with a large number of pores still remaining in the central portion. For the shrinkage (*K*) as low as 20%, sample **5** has no loose texture in its central portion; however, chain-like pore clusters have formed in the sample bulk. With increasing shrinkage, pores of the same size would form in both the central portion and the near-surface layer. The radial forging process completed, both the central portion and the near-surface layer (sample **10**, K = 50%) have uniform pore density and maximal pore size ≤ 1 μm (see Fig. 2 c and d).

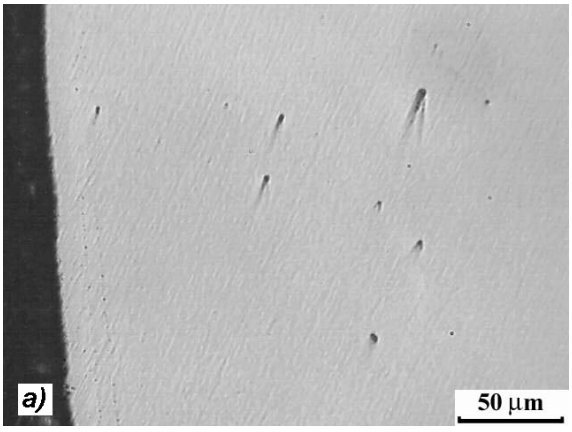

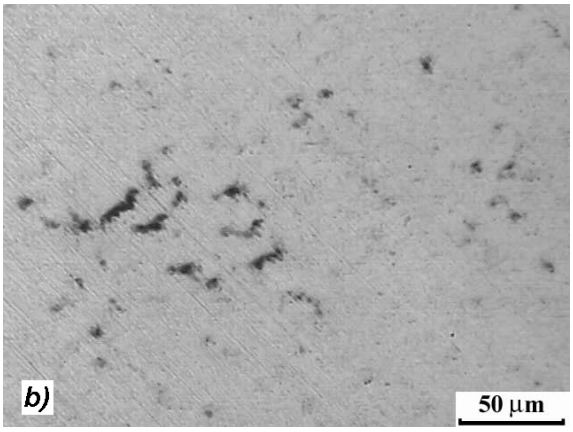

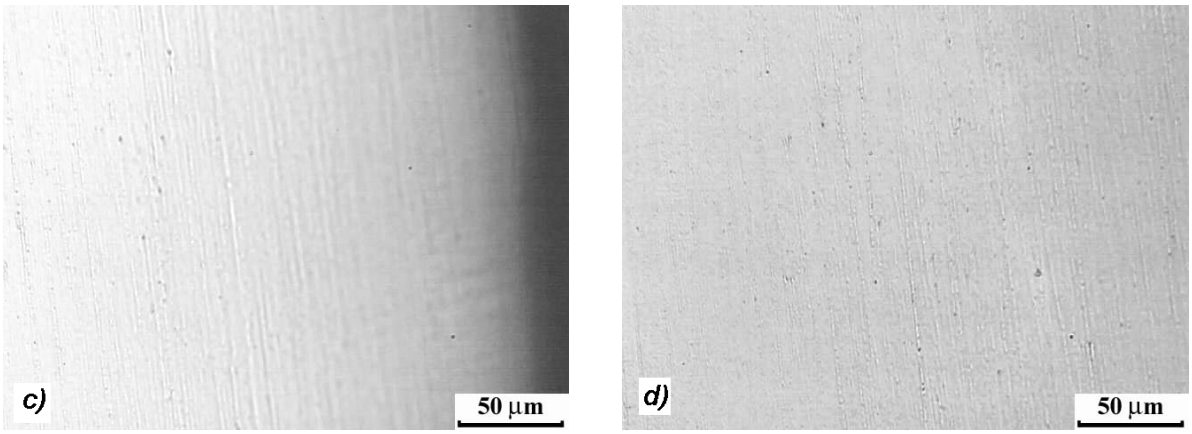

Fig. 2. Porosity in the alloy: (a) sample **1**, surface layers; (b) sample **1**, billet axis; (c) sample **10**, surface layers; (d) sample **10**, billet axis.

The structural and phase state of the alloy was examined metallographically. The results obtained for different *K* values are presented in Fig. 3 a through e. All the metallographic samples have one feature in common: the material along the billet axis has preserved a coarse grain structure. At the preceding process stages (K = 0; Fig. 3 b) a structure containing α- and β-phases formed within the original β-phase grains so that sample **1** has a lamellar coarse grain structure and grain size of 6 units in its central portion (Borisova and co-workers, 1980, Moyiseev, 2001), while the near-surface layer has a more disperse structure and grain size of 4 units. In both the central portion and the near-surface layers the material structure has varying grain sizes (Fig. 3 a). A marked change is observed in the morphology and structural element size of sample **3** (Fig. 1), which was cut from the middle portion of a deformation nucleus after the first pass (K = 17%; ∅20→∅16 mm). With decreasing grain size, transformation of a lamellar structure to a globular structure would occur in both the near-surface layers and along the rod axis (Figs. 3 c and d, respectively). For K = 20%, about 4/5th of the near-surface layer material (sample **5**) acquires a fine-grain globular structure (grain size 2...3 units), while the material in the axial portion (~1/2…3/5) still has a globular structure (grain size 4 units), with the structural components having different sizes.

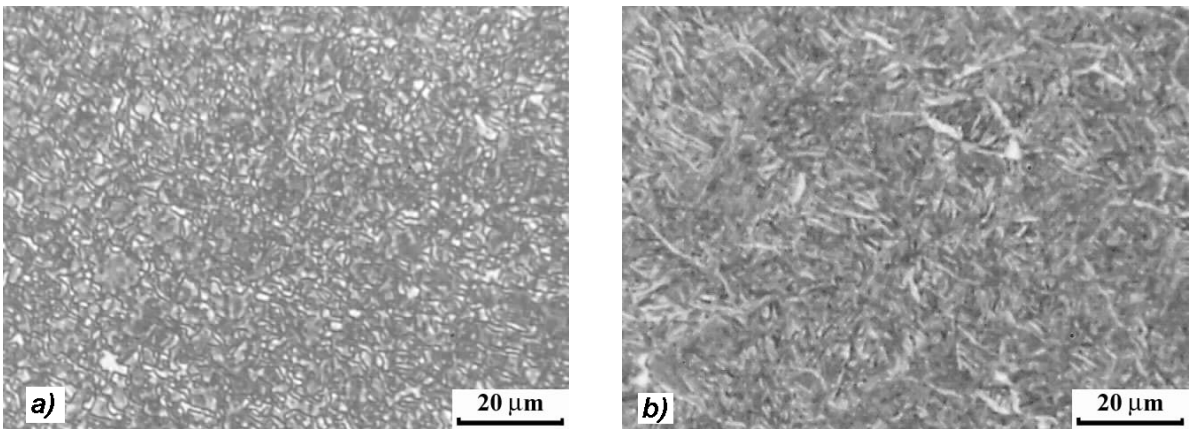

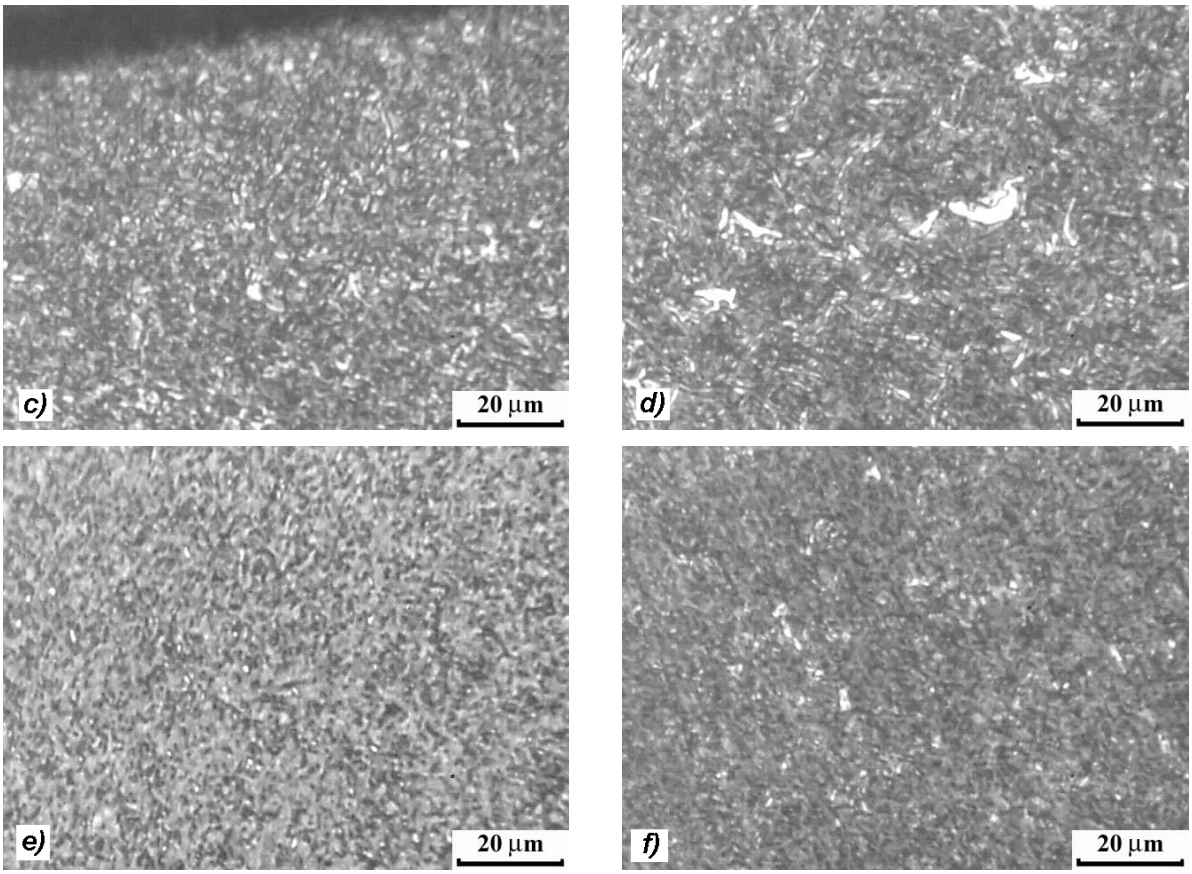

Fig. 3. A gradual decrease in the material's grain size by radial forging: (a) sample **1**, surface layers; (b) sample **1**, billet axis; (c) sample **3**, surface layers; (d) sample **3**, billet axis; (e) sample **10**, surface layers; (f) sample **10**, billet axis

After the second pass (∅16→∅10 mm) samples **7**, **8** and **10** were cut from the billets. The material in these samples has practically the same grain size. The non-uniform globular-lamellar structure observed in the near-surface layers of sample **7** (K = 23%) is found to be replaced by a near-uniform globular structure observed for sample **10** (K = 50%). As is seen from Fig. 3 e, the material in near-surface layers has a uniform globular structure and average grain size < 0.1 μm (sample **10**; grain size 1 unit), while the material along the billet axis (Fig. 3 f) has a non-uniform structure with about 1/4th of grains of a lamellar structure, with the average grain size 0.2…0.5 μm (sample **10**; grain size 2…3 units). It is thus concluded that by radial forging, a globular submicrocrystalline structure would form in the entire volume of (α+β) titanium alloy rod.

3.2 Evolution of fine structure of the material by radial forging

The results of transmission electron microscopy are demonstrated in Figs. 4 through 6. As is seen from Fig. 4 a and b, the original billet microstructure contains colonies of parallel α-phase plates, which are equiaxial within the original β-phase grain and are separated by interlayers of residual β-phase. The α-phase plates and β-phase interlayers have a well-developed dislocation structure, with some 'spotty' structure resulting from poor solubility of alloying elements in the solid α-phase solution. In the near-surface layers there are areas, which have a disperse structure and which are a mixture of α- and β-phases (Fig. 4 c); these are characterized by high dislocation density and inhomogeneous composition. These areas alternate with the remaining fragments of α- and β-phase colonies that had not

ISSN 1313-2539, Published at: http://www.science-journals.eu

disintegrated during the deformation (Fig. 4 d). The structural elements have average cross-section ≤ 0.5 μm.

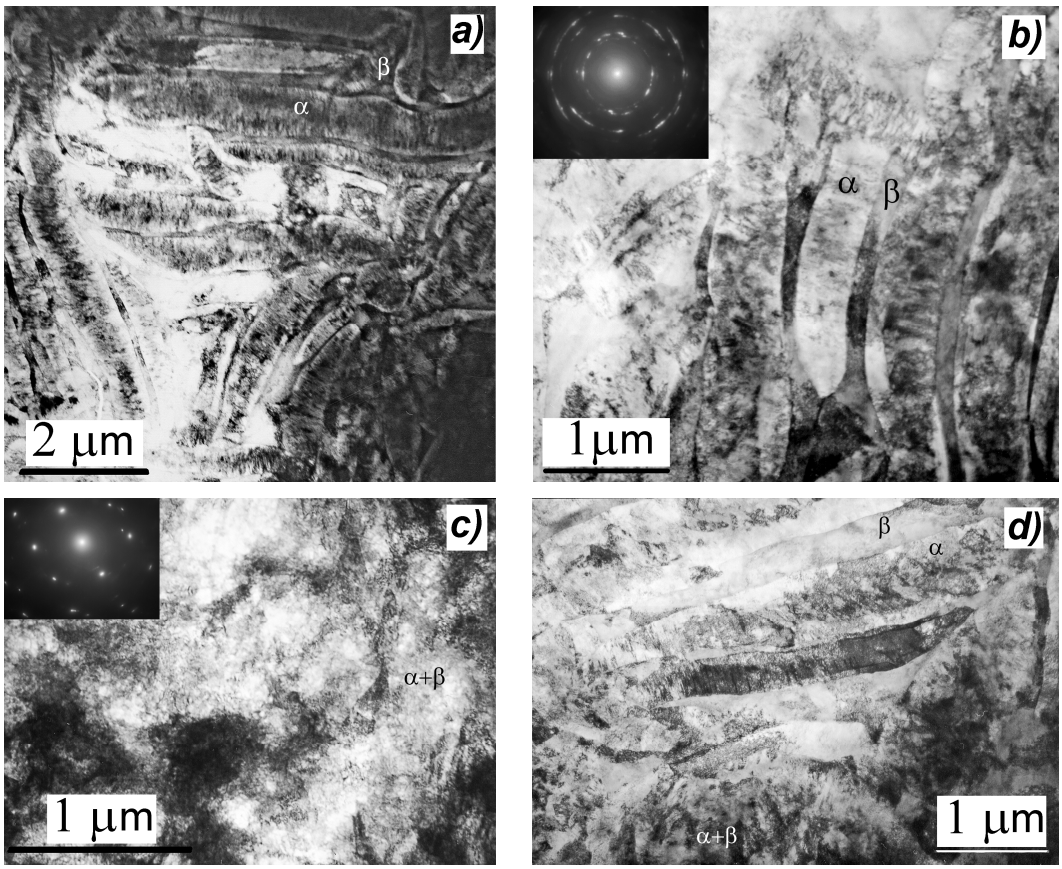

Fig. 4. Microstructure of sample **1**: (a) and (b) billet axis; (c) and (d) surface layers

By radial forging, distortion of *α*-phase plates and *β*-phase interlayers would occur in the originally inhomogeneous billet structure (Fig. 5) as well as disintegration of *α*- and *β*-phase colonies and dispersion of the material structure. The 'spotty' contrast of the light-field image suggests that due to poor solubility of secondary phases, *α*-phase solid-solution precipitates would form within the structural components. For K = 20%, most of the near-surface layer is composed of *α*- and *β*-phases with the average cross-section of structural elements ~ 0.3 μm (Fig. 5 c and d).

As a result of severe plastic deformation, in particular, radial forging, the material undergoes recrystallization; as-treated material has a disperse uniform structure composed of *α*- and *β*-phases, with structural elements having sizes 0.05…0.3 μm (Fig. 6).

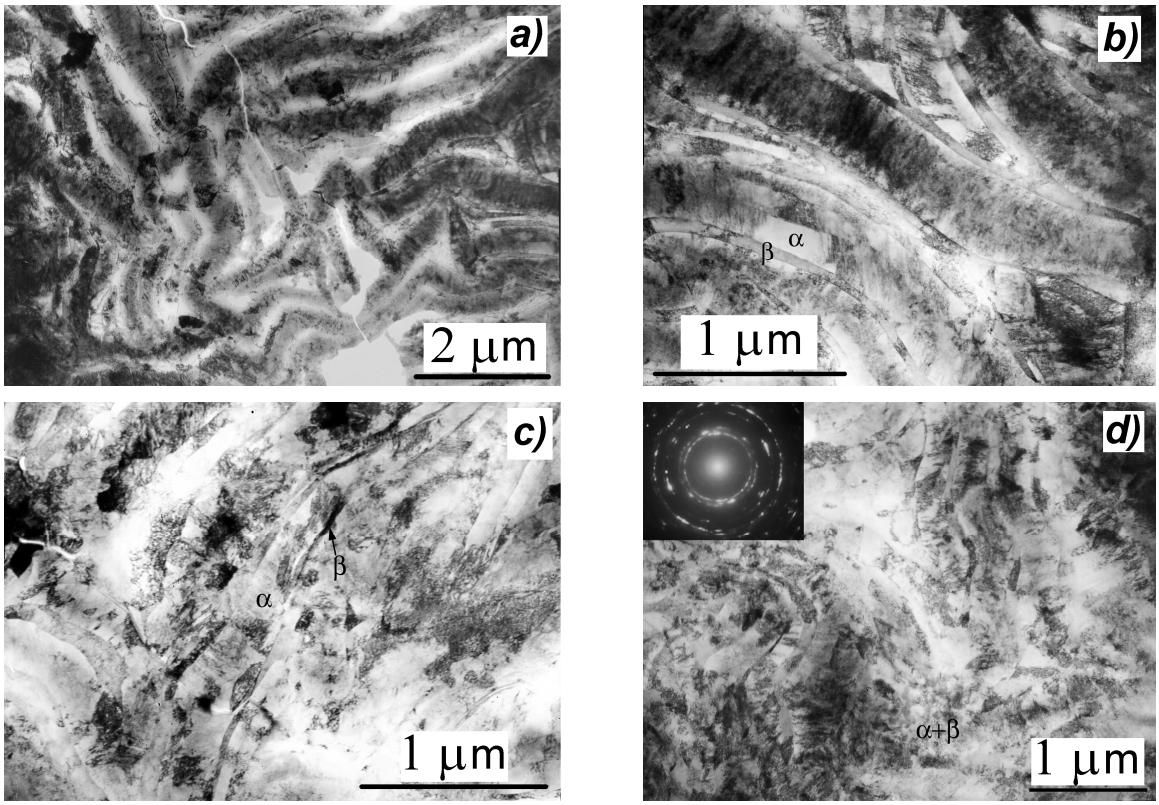

Fig. 5. Microstructure of sample **5**: (a) and (b) on one half of the billet radius; (c) and (d) at 1-mm depth from the billet surface (microdiffraction image suggestive of occurrence of fine disperse α- and β-phases)

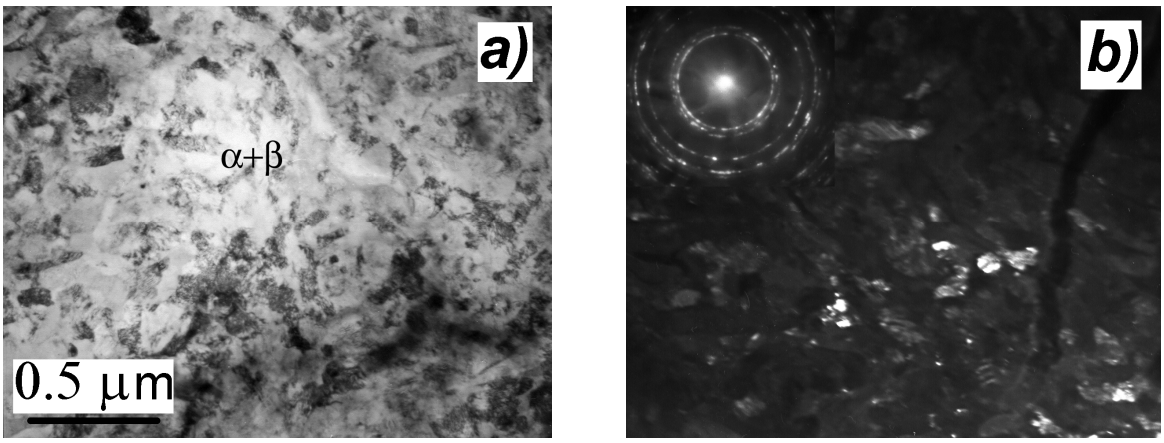

Fig. 6. Microstructure of sample **10** (axial portion): (a) and (b) light- and dark-field images, respectively (microdiffraction image suggestive of fine disperse structure and of occurrence of α- and β-phases)

3.3. X-ray phase analysis

The X-ray phase analysis was performed for samples **2**, **4**, **5**, **8**, **9** and **10**. The X-ray photographs obtained for the test samples are typical for diphase materials. These suggest the presence of hcp α-Ti and bcc β-Ti having the following lattice characteristics: $a = b = 0.29487$ nm, $c = 0.46857$ nm and $a =$

ISSN 1313-2539, Published at: http://www.science-journals.eu

0.3231nm, respectively. A slight discrepancy between the observed data and those reported for pure titanium in, e.g. Zwicker, 1974, must be due to the occurrence of alloying elements dissolved in □- and □- phases.

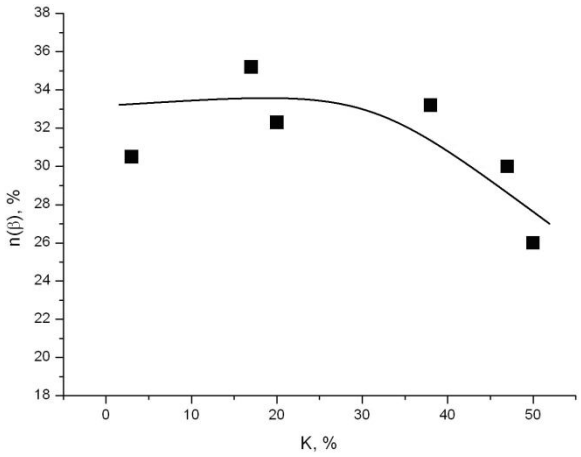

Fig. 7. Volume fraction of β-phase vs shrinkage by radial forging

Of particular importance is a variation in the phase composition of titanium alloy VT16 due to radial forging, in particular, in the volume fraction of bcc β-phase (Fig. 7). This finding is based on the ratio of experimental and calculated (Lysak and Nikolin, 1975) intensities of the spectral lines 102 and 200, which were observed for different K values for α- and β-phase, respectively. It follows from Fig. 7 that for $K \leq 20\%$ (beginning of forging), the volume fraction of β-phase is ~1/3, which exceeds the allowable level specified for the studied alloy (Ilyin and co-workers, 2009). For $K = 50\%$, the volume fraction of β-phase decreases to the specified allowable level of ~1/4. The above variation in the volume fraction of β-phase is due to the deformation-induced martensitic transformation $\beta \rightarrow \alpha''$ that takes place in the course of radial forging. It is found that although original sample **2** contains an insignificant amount of martensitic α''-phase, the stable α-phase prevails in the bcc structure. The volume fraction of meta-stable α''-phase in samples **9** and **10** is comparable to that of α-phase.

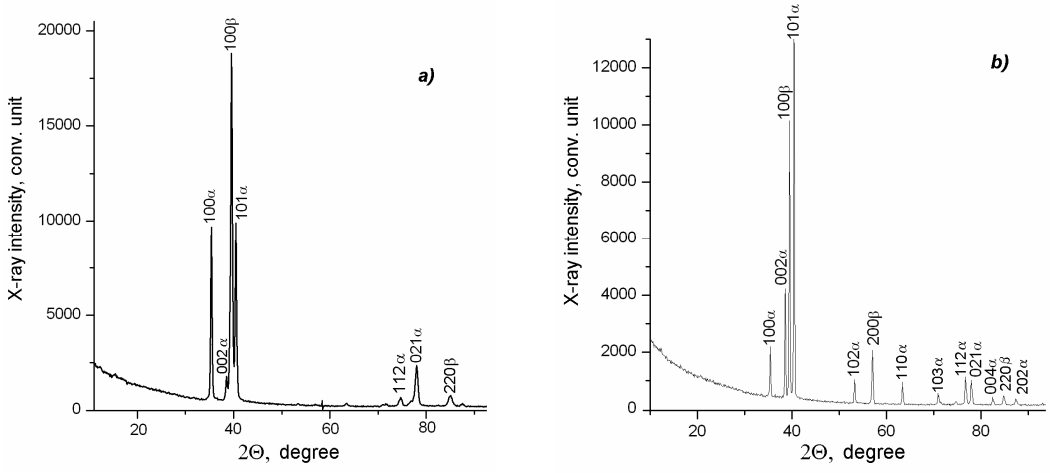

Fig. 8. X-ray diffraction patterns of samples **5** (a) and **10** (b)

As a result of radial forging, the texture that had formed by hot pressing is eliminated (Fig. 8 a), which is suggested by the similarity between the diffraction patterns obtained for sample **10** and annealed fine grain material (Fig. 8*b*). The former shows 002 and 004 lines of α-phase, which are absent from the diffraction patterns obtained for other samples worked by radial forging to lower K values.

It should be noted that the rods produced by radial forging have adequate geometric parameters and a satisfactory degree of surface roughness. Compare the surface roughness 3…8 μm and the ovality < 30 μm against the respective values of ≤ 10 μm and < 40 μm that are specified for rods ∅10 mm.

4. CONCLUSION

The data presented herein suggests that by cold radial forging, the original inhomogeneous lamellar structure of rods manufactured from (α+β) titanium alloy would transform into near-homogeneous globular submicrocrystalline structure having grain size 0.05…0.3 μm (1…2 conventional units). Moreover, as-worked material has an optimal ratio of α- and β-phase (by volume). The finished items (rods) have satisfactory surface roughness and adequate geometrical dimensions, which makes unnecessary their mechanical treatment. Thus, the application of cold radial forging process holds much promise for development of new highly effective technology for the manufacture of billets from the alloy Ti-3Al-4.5V-5Mo, which are intended for the production of hardware by cold-work.

ACKNOWLEDGEMENTS:

The present work is supported by RFBR through grant No. 09-08-00498.

REFERENCES

1. Beckert M., Klemm H. *Handbuch der metallographischen Ätzverfahren*. VED Deutscher Verlag für Grundstoffindustrie. (Leipzig) 1984.
2. Borisova, E.A., Bochvar G.A. *Metal Science: Titanium Alloys*. (Moscow) Metallurgy; 1980.
3. Bratukhin, V.A. *Tekhnologiya mashinostroeniya* 2009; 12: 33-36 (in Russian).
4. Collings E.W. *The physical metallurgy of titanium alloys*. American Society of Metals, Metals Park, OH 44073; 1984.
5. Guinier A. *Théorie et technique de la radiocristallographie*. DUNOD. (Paris) 1956.
6. Ilyin, B.A., Kolachev, I.S., Polkin, A.A. *Titanium alloys. Composition – Structure – Properties*. (Moscow) VILS-MATI; 2009 (in Russian).
7. Jaffee R.I. *Progress in Metal Physics. Vol. VII*. Pergamon Press.(London, New York, Paris, Los Angeles) 1958; 77-191.
8. Lysak L.I., Nikolin, B.I. *Physical Principles of Thermal Treatment of Steels. (*Kiev) Tekhnika; 1975 (in Russian).
9. Moyiseev, V.N. *Metal Science and Heat Treatment* 2001; 2: 28-32.
10. Muravyov, V.I., Bakhmatov, P.V., Dolotov, B.I. *Long-Term Reliability of Constructions from Titanium Alloys*. (Moscow) Ecom; 2009 (in Russian).
11. Shorokhov E.V., Zhgiliev I.N., Gunderov D.V., Gurov A.A.. *Proc. Int. Conf. "Shock waves in condensed matter"* (St. Petersburg) 2006; 281-83.
12. Tomas G., Goringe M.J. *Transmission electron microscopy of materials*. John Wiley & Sons. (New York, Chichester, Brisbane, Toronto) 1979.
13. Zwicker U. *Titanium and its alloys*. Springer Verlag; 1974.